CHINESE JOURNAL OF PHYSICS VOL. 52, NO. 5 October 2014

Magnetic Field Induced Exciton Binding Energy in a Strained $GaAs_{1-x}P_x/GaAs_{0.6}P_{0.4}$ Quantum Dot

Ada Vinolin,[1] A. John Peter,[2,*] and Chang Kyoo Yoo[3]

[1]*Department of Physics, Madurai Kamaraj University College, Alagarkoil Road, Madurai-625 002, India*

[2]*Department of Physics, Government Arts College, Melur-625 109, Madurai, India*

[3]*Center for Environmental Studies / Green Energy Center, Department of Environmental Science and Engineering, College of Engineering, Kyung Hee University, Seocheon-dong 1, Giheung-gu, Yongin-Si, Gyeonggi-Do, 446-701, South Korea*

(Received July 3, 2012; Revised March 18, 2013)

The exciton binding energy with geometrical confinement and a phosphorous alloy content in a cylindrical $GaAs_{1-x}P_x/GaAs_{0.6}P_{0.4}$ ($x \leq 0.3$) strained quantum dot is investigated. The band offset is calculated using model solid theory. The strained $GaAs_{1-x}P_x/GaAs_{0.6}P_{0.4}$ quantum dot has the strong built-in electric field due to the spontaneous and piezoelectric polarizations. Numerical calculations are performed using a variational procedure within the single band effective mass approximation with the magnetic field. The magnetic field induced interband emission energy of the strained GaAsP quantum dot is investigated for various phosphorous alloy contents. The exciton oscillator strength and the exciton lifetime for radiative recombination as a function of the dot radius with the effect of the magnetic field strength and the phosphorus concentration are computed.

DOI: 10.6122/CJP.20130513 PACS numbers: 73.21.Fg, 42.65.An, 71.38.-k

I. INTRODUCTION

Group III-V semiconducting heterostructures are quite interesting as they find some potential applications in fabricating optical devices, such as optical switches and phase modulators [1]. Guided wave switching can be modulated when there is a change in some non-linear optical properties, such as the absorption coefficients and refractive index changes [2]. These non-linear optical properties are important for laser design using GaAs compound semiconductors [3, 4]. Compressive and tensile strain occurs, leading to a change of the energy-band structure of the semiconductor layers in the heterostructures [5, 6]. Large non-linear optical properties can be achieved due to the strain-induced internal electric field with piezoelectrical semiconducting materials [7].

The energy levels in these heterostructures not only depend on the composition of the barrier and dot size but also on the lattice constants of the dot and barrier material. Eventually, this will affect the valence and conduction bands. It is well known that a typical III-V semiconductor such as GaAs experiences a compressive strain, whereas AsGaP experiences

*Electronic address: a.john.peter@gmail.com

tensile strain [8], and this property makes a GaAs/AsGaP heterostructure more interesting for the invention of lasers emitting in the infrared red regions. Energies of the band-to-band transitions with the quantum-confinement subbands have been investigated from the photoreflection spectra of the strained short-period $GaAs/GaAs_{0.6}P_{0.4}$ superlattice [9]. The energy-band diagram of GaAs/GaAsP heterostructures has been calculated assuming the potential jump in the conduction band to be smaller than the potential jump in the valence band [10]. The PL spectra both for the GaAs/GaAsP strained barrier and strained-well single quantum well structures were obtained earlier [11, 12]. Tensile-strained GaAsP quantum wells embedded in AlGaAs large optical cavity structures were investigated [13]. The growth and the related photoluminescence properties of the tensile-strained GaAsP/GaInP quantum wells have been discussed, and the effects of tensile strain on the optical properties have been investigated [14]. This tensile strain can be used to modify the energy dispersion of the low dimensional semiconductor band structure in order to improve its optical characteristics, such as the nonradiative recombination processes [15].

In the present work, we have considered a $GaAs_{1-x}P_x$ ($x < 0.3$) quantum dot embedded on a $GaAs_{0.6}P_{0.4}$ barrier. The effect of the magnetic field and the phosphorous alloy content on the exciton binding energy is investigated, taking into account the geometrical confinement. We have included the strong built-in electric field due to the spontaneous and piezoelectric polarizations in the Hamiltonian. Numerical calculations are performed using a variational procedure within the single band effective mass approximation with the magnetic field. The effect of the magnetic field, the geometrical confinement, and the phosphorous alloy content on the interband emission energy and the oscillator strength of a strained $GaAs_{1-x}P_x/GaAs_{0.6}P_{0.4}$ quantum dot is investigated. In Section II, we briefly describe the method used in our calculation. And the results and discussion are presented in Section III. A brief summary is presented in the last section.

II. THEORY AND MODEL

The magnetic field induced binding energy of an exciton and thereby some nonlinear optical properties are studied in a cylindrical $GaAs_{1-x}P_x/GaAs_{0.6}P_{0.4}$ ($1 - x \leq 0.4$) strained quantum dot incorporating the effect of a piezoelectric field. The cylindrical quantum dot (GaP) is considered with the radius R surrounded with the barrier height H of a larger band gap energy, $GaAs_{1-x}P_x$. The Hamiltonian of a magneto exciton in the $GaAs_{1-x}P_xP/GaAs_{0.6}P_{0.4}$ cylindrical quantum dot consisting of a single electron part (H_e), the single hole part (H_h), and the Coulomb interaction term between electron-hole pair, within the effective mass-approximation, is given by

$$H_{\text{exc}} = \sum_{j=e,h} \left[\frac{1}{2m_j(E)} \left(\vec{p}_j - \frac{q\vec{A}_j}{c} \right)^2 \pm \sigma_z \mu_B g_j(E) B + V(r) \right] - \frac{e^2}{\varepsilon \left| \bar{r} \right|} \pm |e| \, Fz, \qquad (1)$$

where $\vec{p}$ is the momentum operator, $\vec{A}$ is the vector potential, q is the charge ($-e$ for electrons and $+e$ for holes), $|\bar{r}| = |\bar{r}_e - \bar{r}_h|$ denotes the relative distance between the electron

and the hole, $V(r)$ is the confinement potential of the exciton, F is the effective electric field due to the piezoelectric effect and ε is the dielectric constant of the material inside the quantum dot, μ_B is the Bohr magneton, and σ is the spin taken as $\pm 1/2$ [17]. The z-component of the spin has been taken as $\pm 1/2$ for simplicity for holes. The parameters used in our calculations are given in Table I.

TABLE I: Material parameters* used in the calculations.

Parameter	$GaAs_{0.9}P_{0.1}$	$GaAs_{0.8}P_{0.2}$	$GaAs_{0.7}P_{0.3}$	$GaAs_{0.6}P_{0.4}$
E_g^{Γ} (eV)	1.543	1.666	1.793	1.923
m_e (m_0)	0.085	0.104	0.122	0.14
Δ (meV)	0.314	0.288	0.262	0.236
ε	12.93	12.72	12.52	12.32
$_{mhh}$	0.385	0.43	0.475	0.52
$_{mlh}$	0.097	0.102	0.106	0.111
C_{11} (GPa)	12.104	12.328	12.552	12.776
C_{12} (GPa)	5.467	5.554	5.641	5.728
$E_{v,av}$ (eV)	−6.963	−7.007	−7.05	−7.098
a_c (eV)	−7.167	−7.164	−7.161	−7.158
a_v (eV)	−1.214	−1.268	−1.322	−1.376
a_c (eV)	−7.167	−7.164	−7.161	−7.158
γ_1	6.575	6.3	6.025	5.75
γ_2	1.939	1.778	1.617	1.456
Lattice constant (Å)	5.633	5.613	5.593	5.572

*Ref. [23, 31]

The Hamiltonian of the electron (hole) in cylindrical co-ordinates, in the influence of a magnetic field, is given by

$$H_{\text{exc}} = -\sum_{j=e,h}\left(\frac{\hbar^2}{2m_j(E)}\left[\frac{\partial^2}{\partial\rho_j^2}+\frac{1}{\rho_j}\frac{\partial}{\partial\rho_j}+\frac{1}{\rho_j^2}\frac{\partial^2}{\partial\varphi^2}+\frac{\partial^2}{\partial z_j^2}\right]\mp\frac{i\hbar eB}{2m_j(E)c}\frac{\partial}{\partial\phi}+\frac{e^2B^2\rho_j^2}{8m_j(E)c^2}\right.$$
$$\left.+V(\rho_j,z_j)\right)\pm\sum_{j=e,h}\sigma_z\mu_B g_j(E)B-\frac{e^2}{\varepsilon\sqrt{\rho_{eh}^2+(z_e-z_h)^2}}\pm|e|\,Fz, \qquad (2)$$

where the subscript $j = e, h$ refers the electron or hole. The electron effective mass m_e^* is

given by

$$m_e^* = \begin{cases} m_I^*, & \rho \le R \\ m_{II}^*, & \text{otherwise} \end{cases} \tag{3}$$

m_I^* denotes the electron effective mass of $GaAs_{1-x}P_x$, and m_{II}^* denotes the electron effective mass of the outer material, $GaAs_{0.6}P_{0.4}$. Since it has a large influence on the electron energy levels in a semiconductor quantum dot, especially for the narrow dots, the material dependent effective mass has been used in this calculation [18].

The energy dependent effective mass is given by

$$\frac{1}{m(E)} = \frac{1}{m(0)} \frac{E_g(E_g + \Delta)}{(3E_g + 2\Delta)} \left[\frac{2}{E + E_g} + \frac{1}{E + E_g + \Delta} \right], \tag{4}$$

where ε is the dielectric constant of $GaAs_{1-x}P_x$, E denotes the electron energy in the conduction band, $m(0)$ is the conduction band effective mass, E_g and Δ are the main band gap and spin-orbit band splitting, respectively, and

$$g(E) = 2 \left[1 - \frac{m_0}{m(E)} \frac{\Delta}{3(E_g + E) + 2\Delta} \right] \tag{5}$$

is the effective Landé factor of the electron [19]. In Eq. (5), m_0 denotes the free electron mass.

The strain effects will induce an extra potential field, V_{strain}. For the strained quantum dot nanostructure, the confinement potential can be written as a sum of energy offsets of the conduction band (or valence band) and the strain-induced potential.

The electron (hole) confinement potential $V(\rho_j)$ due to the band offset in the $GaAs_{1-x}P_x/GaAs_{0.6}P_{0.4}$ quantum dot structure is given by

$$V(\rho_j) = \begin{cases} 0, & \rho_j \le R \\ V_0, & \text{otherwise} \end{cases} \tag{6}$$

where

$$V_0 = Q_c \Delta E_g^{\Gamma} \tag{7}$$

is the barrier height, Q_c is the conduction band offset parameter, and the band offset ratio (ΔE_c : ΔE_v) is assumed to be 80:20 [20]. ΔE_g^{Γ}, the band gap difference between the quantum dot and the barrier at the Γ-point is given by [21, 22]

$$\Delta E_g^{\Gamma} = \Delta E_g^{\Gamma}(\text{unstrained}) + \delta E_{c(v)c}, \tag{8}$$

with [23]

$$\Delta E_g^{\Gamma}(\text{unstrained})(\text{eV}) = 1.424 + 1.174x + 0.186x^2, \tag{9}$$

$$\delta E_c = 2a_c\varepsilon_{xx}(C_{11} - C_{12})/C_{11}, \tag{10}$$

and

$$\delta E_v = 2a_v\varepsilon_{xx}(C_{11} - C_{12})/C_{11} + b\varepsilon_{xx}(C_{11} + 2C_{12})/C_{11}, \tag{11}$$

where $a_{c(v)}$ is the deformation potential constants of the conduction (valence) band, b is the uniaxial strain; the strain in the layer is given by $\varepsilon_{xx} = \frac{a_0 - a}{a}$, where a_0 and a are the lattice parameters of the dot and the barrier, respectively. The strain causes a shift in the conduction band, resulting in an increase in the band gap of the dot and a decrease in the band gap of the barrier, the uniaxial strain removes the degeneracy between the heavy hole and light hole subband energy in the valence band.

The V_e and V_h are calculated using the following expression:

$$V_c = E_c^B - E_c^D, \tag{12}$$

$$V_h = E_v^B - E_v^D, \tag{13}$$

where E_c^D and E_v^D are the energies of the conduction and heavy hole bands in the barrier dot, and E_c^B and E_v^B are the energies of the conduction and heavy hole bands in the inner dot.

The exciton binding energy is reduced when the piezoelectric effect is included, and the expression of piezo-electric field is given by

$$F = \frac{2d_{31}}{\varepsilon}\left(C_{11} + C_{12} - \frac{2C_{13}^2}{C_{33}}\right)\varepsilon_{xx}, \tag{14}$$

where d_{31} is the piezoelectric constant of $GaAs_{1-x}P_x$, ε is the dielectric constant of the material inside the quantum dot, C_{11}, C_{12}, C_{13}, and C_{33} are the elastic stiffness constants, and ε_{xx} is the in-plane component of the strain tensor, given by

$$\varepsilon_{xx} = \varepsilon_{yy} = \frac{a_{\text{out}} - a_{\text{in}}}{a_{\text{in}}}, \tag{15}$$

where a_{out} and a_{in} are the lattice constants of the $GaAs_{1-x}P_x$ and $GaAs_{0.6}P_{0.4}$ material, respectively.

The sub-band energy is obtained using the wave function as

$$\psi_j = \begin{cases} A_1\cos(k_1\rho), & \rho_j \le R \\ B_1\exp(-k_2\rho), & \rho_j > R \end{cases} \tag{16}$$

where $k_1 = \sqrt{2m^*E_1/\hbar^2}$, $k_2 = \sqrt{2m^*(V_0 - E_1)/\hbar^2}$, and A_1 and B_1 are normalization constants. Eq. (16) fixes the values of k_1 and k_2 for the lowest values of E_1. By matching the wave functions and their derivatives at the boundaries of the dot and along with the normalization, we fix all the constants except the variational parameters.

The heavy-hole and light-hole masses in terms of the Luttinger parameters, γ_1 and γ_2, (Table I) are given by [24]

$$\frac{m_0}{m^*_{hh}} = \gamma_1 - 2\gamma_2, \tag{17}$$

$$\frac{m_0}{m^*_{lh}} = \gamma_1 + 2\gamma_2, \tag{18}$$

where m_0 is the free electron effective mass.

The Schrödinger equation is solved variationally by finding $\langle H \rangle_{\min}$, and the binding energy of the exciton in the quantum dot is given by the difference between the energy with and without the Coulomb term. First, we concentrate on the calculation of the electronic structure of the $GaAs_{1-x}P_x/GaAs_{0.6}P_{0.4}$ quantum dot system by calculating its subband energy E_1 with the inclusion of the magnetic and subsequently the exciton binding energy. And then, by using the density matrix approach within a two-level system approach, the explicit expressions for the nonlinear optical properties, such as the nonlinear optical absorption and the changes of refractive index, are computed in the saturation limit. Considering the correlation of the electron-hole relative motion, the trial wave function can be chosen as

$$\Psi(\bar{r}_e, \bar{r}_h) = \psi_e(\rho_e)\psi_h(\rho_h)\exp(-\gamma\rho^2/4)e^{-\delta\rho^2}e^{-\beta z^2}, \tag{19}$$

where ψ_e and ψ_h are the electron and hole wave function in the quantum dot, respectively, as given in Eq. (15). The above equation describes the correlation of the electron-hole relative motion. δ and β are variational parameters responsible for the in-plane correlation and the correlation of the relative motion in the z-direction, respectively [25]. These two variational parameters are responsible for the anisotropy of the cylindrical nature of the quantum dots. And hence, it is believed that this type of Gaussian wave function is a suitable approximation in a quantum limit region [26].

The ground state energy of the exciton in the $GaAs_{1-x}P_x/GaAs_{0.6}P_{0.4}$ quantum dot in the external magnetic field, E_{exc}, is obtained by minimizing the expectation value of H_{exc} with respect to the variational parameters using Eq. (15). The ground state energy of the exciton in the $GaAs_{1-x}P_x/GaAs_{0.6}P_{0.4}$ quantum dot is calculated by using the following equation

$$E_{\text{exc}} = \min_{\gamma,\delta,\beta} \frac{\langle \psi_e | H_{exc} | \psi_h \rangle}{\langle \psi_e | \psi_h \rangle}. \tag{20}$$

The exciton binding energy in the presence of a magnetic field is given by

$$E_B(B) = E_e + E_h + \gamma - E_{\text{exc}}(B). \tag{21}$$

We define $\gamma = \frac{\hbar\omega_c}{2Ry^*}$, where R^*_y is the effective Rydberg energy and ω_c is the cyclotron frequency, and the magnetic field induced interband emission energy $E_{ph}(B)$ associated with the exciton is calculated using the following equation:

$$E_{ph}(B) = E_e + E_h + \gamma + E_g - E_{\text{exc}}(B), \tag{22}$$

where E_e and E_h are the confinement energies of the electron and hole, respectively. E_g is the band gap energy of the $GaAs_{1-x}P_x/GaAs_{0.6}P_{0.4}$ quantum dot.

The oscillator strength of the exciton ground state is given by [27]

$$f_{\text{exc}} = \frac{2P^2}{m_0(E_{\text{exc}} - E)} \left|\psi(\bar{r}_e - \bar{r}_h)d\tau\right|^2, \tag{23}$$

where P is the matrix element, m_0 is the bare electron mass, E_{exc} is the exciton binding energy, and E is the ground state energy of the electron and hole. The value of $P^2/2m_0$ is assumed to 1 eV.

III. RESULTS AND DISCUSSION

Numerical calculations have been carried out to find the exciton binding energy, the interband emission energy, and the oscillator strength in a strained $GaAs_{1-x}P_x/GaAs_{0.6}P_{0.4}$ quantum dot in the presence of a magnetic field for different phosphorous content. The material parameters used are given in Table I. The atomic units have been followed in the determination of the electronic charges and the wave functions, in which the electronic charge and Planck's constant have been assumed as unity. All our calculations of the exciton binding energy have been carried with the heavy hole mass, as the heavy excitons are more common in experimental results.

Fig. 1 shows the variation of the magnetic field as a function of the measure of the magnetic field for various concentrations of the phosphorous alloy content in a $GaAs_{1-x}P_x$ quantum dot. It is observed that the linear variation of the magnetic field as a function of the measure of the magnetic field is found for all the phosphorous content, and this variation is more dominant when the phosphorous alloy content becomes more and more in the quantum dot. The following magnetic field strength is found for different concentrations. When $\gamma = 1$ it is 7.875 T for $x = 0.1$, 10.75 T for $x = 0.2$, 14.34 T for $x = 0.3$, and 18.43 T for $x = 0.4$. All the calculations are carried out using the reduced mass and the concentrated dependent dielectric constants.

Fig. 2 displays the variation of the exciton binding energy as a function of the dot radius for three different concentrations of the phosphorus content in a $GaAs_{1-x}P_x/GaAs_{0.6}P_{0.4}$ quantum dot in the absence of magnetic field strength, and the insert figure shows the variation of the exciton binding energy as a function of the dot radius for different magnetic field strengths for a constant x in the $GaAs_{0.9}P_{0.1}/GaAs_{0.6}P_{0.4_{\text{out}}}$ quantum dot. In all the cases, the exciton binding energy increases with a decrease of the dot radius, reaching a maximum value and then decreases when the dot radius decreases further. The Coulomb interaction between the electron and hole is increased, which ultimately causes a decrease in the binding energy when the dot radius decreases. The binding energy decreases further as the dot radius approaches zero, since the confinement becomes negligibly small and in the finite barrier problem the tunneling becomes huge. Also, the contribution of confinement is dominant for smaller dot radii, making the electron unbound, and ultimately it tunnels through the barrier. This is in agreement with the results of other

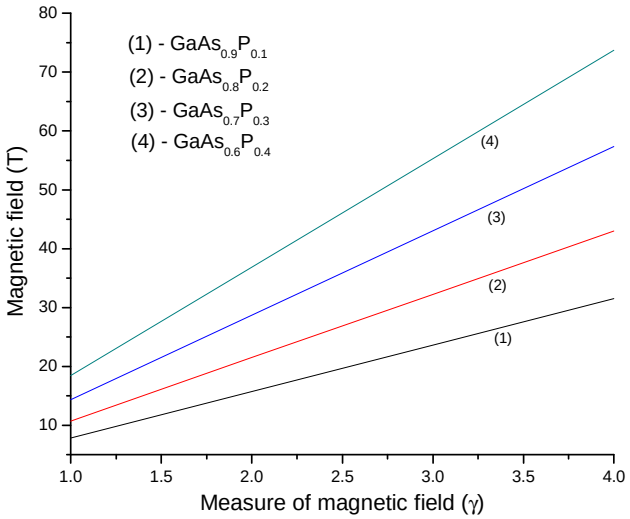

FIG. 1: Variation of the magnetic field strength as a function of the measure of the magnetic field for various concentrations of P in a $GaAs_{1-x}P_x$ quantum dot. When $\gamma = 1$ it is 7.875 T for $x = 0.1$, 10.75 T for $x = 0.2$, 14.34 T for $x = 0.3$, and 18.43 T for $x = 0.4$.

investigators [27, 28]. Moreover, we find that the exciton binding energy increases with the phosphorous alloy content for all the dot radii. That is because the barrier height increases when the phosphorous concentration is increased in the $GaAs_{1-x}P_x/GaAs_{0.6}P_{0.4}$ quantum dot.

This behaviour is observed for all the values of the magnetic field. Further, we notice that the binding energy increases with the magnetic field for all the dot radii. This is due to the extra confinement of the magnetic field being raised when the wave functions are squeezed, and it is observed that the effect of the magnetic field will have more influence on the bigger dot radius than the smaller ones. Moreover, we notice that the binding energy is more for smaller dot radii than the larger size, due to the additional spatial confinement and addition of phosphorus content making the lattice constant of GaAsP smaller than that of GaAs [14]. A similar trend is observed for all the phosphorus content.

In Fig. 3, we present the variation of shift in the exciton binding energy as a function of the magnetic field strength for three different phosphorus contents of an 80 Å radius of $GaAs_{1-x}P_x/GaAs_{0.6}P_{0.4}$ quantum dot. In all the cases, a linear variation of the binding energy with the magnetic field is observed, however, this variation in the binding energy has more influence for the higher phosphorous concentrations and magnetic field. That is because of the enhancement of the exciton binding energy with an increase of phosphorous alloy content and the confinement due to the magnetic field.

The variation of the interband emission E_{ph} as a function of the dot radius for various

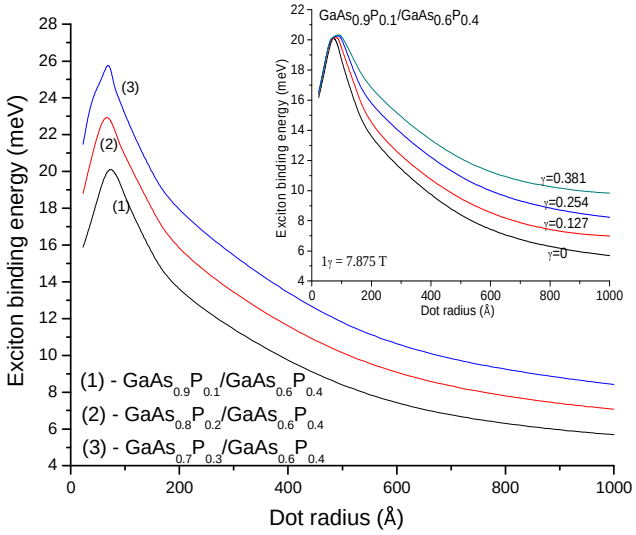

FIG. 2: Variation of the exciton binding energy as a function of the dot radius for three different concentrations of the phosphorus content in a $GaAs_{1-x}P_x/GaAs_{0.6}P_{0.4}$ quantum dot in the absence of magnetic field strength; the insert figure shows the variation of the exciton binding energy as a function of the dot radius for different magnetic field strengths for a constant x in the $GaAs_{1-x}P_x/GaAs_{0.6}P_{0.4}$ quantum dot.

magnetic field strengths in a $GaAs_{1-x}P_x/GaAs_{0.6}P_{0.4}$ quantum dot for $x = 0.1$ is shown in Fig. 4, and the insert figure shows the interband emission energy as a function of the dot radius for three different phosphorus concentrations in the $GaAs_{1-x}P_x/GaAs_{0.6}P_{0.4}$ quantum dot in the absence of a magnetic field. In all the cases, it is observed that the interband emission energy decreases monotonically as the radius of the dot is increased. This is due to the confinement of the electron-hole with respect to the in-plane when the dot radius is increased. This representation clearly brings out the quantum size effect. Moreover, the interband emission energy increases with the magnetic field strength. At present we don't have any experimental data to compare to our results. Moreover, the enhancement of the interband emission energy with the phosphorous alloy content is observed for all the dot radii. This is due to the increase in the binding energy with the phosphorus alloy content.

In Fig. 5, we present the variation of the oscillator strength as a function of the dot radius for various magnetic field strengths in a $GaAs_{0.9}P_{0.1}/GaAs_{0.6}P_{0.4}$ quantum dot. It is observed that the oscillator strength increases with the dot radius. The radiative life time can be calculated as [29]

$$\tau = \frac{2\pi\varepsilon_0 m_0 c^3 h^2}{\sqrt{\varepsilon} e^2 E_{\rm exc}^2 f}, \tag{24}$$

where f is the oscillator strength, $E_{\rm exc}$ is the exciton binding energy, and all the other

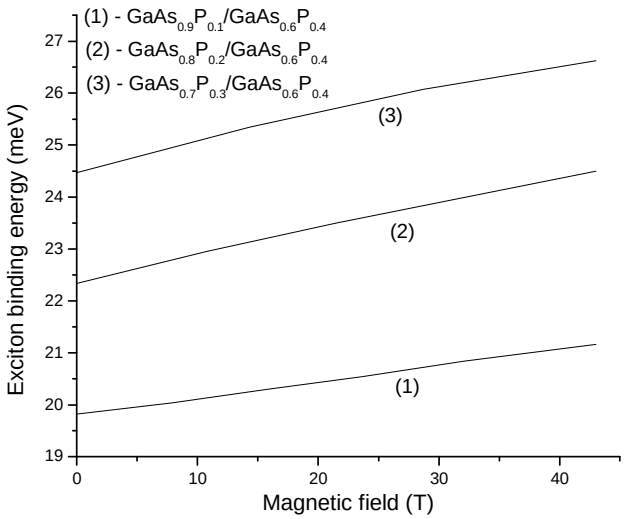

FIG. 3: Variation of shift in exciton binding energy as a function of the magnetic field strength for three different phosphorus contents of an 80 Å, $GaAs_{1-x}P_x/GaAs_{0.6}P_{0.4}$ quantum dot.

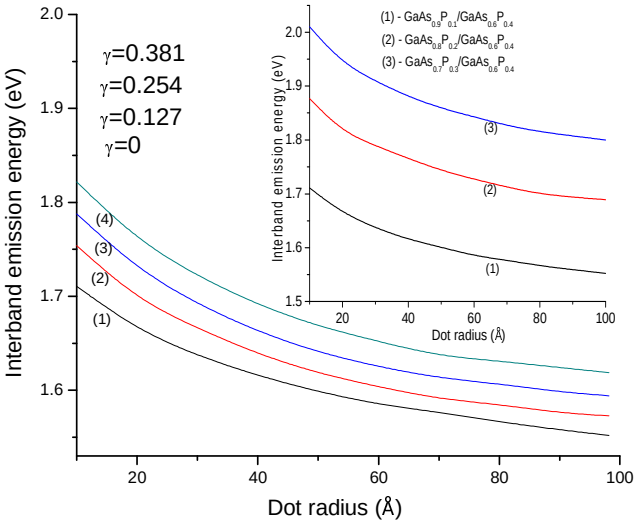

FIG. 4: Variation of interband emission E_{ph} as a function of dot radius for various magnetic field strengths in a $GaAs_{1-x}P_x/GaAs_{0.6}P_{0.4}$ quantum dot for $x = 0.1$; the insert figure shows the interband emission energy as a function of the dot radius for three different phosphorus concentrations in the $GaAs_{1-x}P_x/GaAs_{0.6}P_{0.4}$ quantum dot in the absence of a magnetic field.

parameters are universal physical constants. The envelope function brings out that this considerably reduces the overlap between their wave-functions and increases the radiative decay time when the dot radius increases [30]. The dielectric and mass mismatch in the quantum dot enhance this effect.

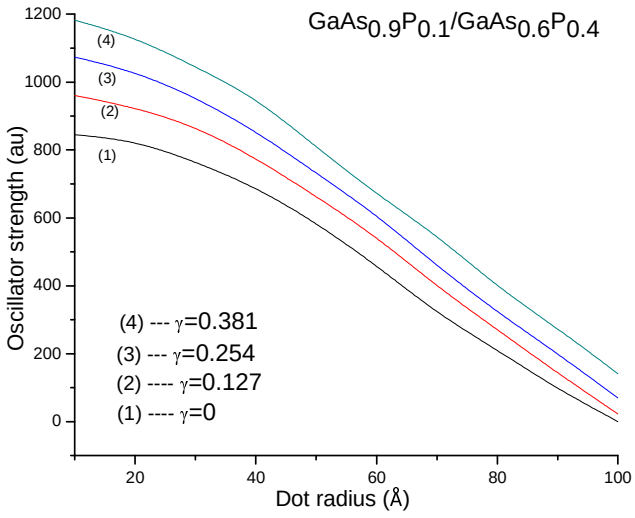

FIG. 5: Variation of oscillator strength as a function of dot radius for various magnetic field strengths in a $GaAs_{0.9}P_{0.1}/GaAs_{0.6}P_{0.4}$ quantum dot.

In conclusion, the effects of a magnetic field, spatial confinement, and the phosphorus alloy content of an exciton confined in a $GaAs_{1-x}P_x/GaAs_{0.6}P_{0.4}$ quantum dot have been discussed. Here, we have considered a quantum dot of $GaAs_{1-x}P_x$ ($x < 0.3$) embedded on a $GaAs_{0.6}P_{0.4}$ as barrier. In all the calculations, we have included the strong built-in electric field due to the spontaneous and piezoelectric polarizations. Numerical calculations are performed using a variational procedure within the single band effective mass approximation by the magnetic field strength. The band offset has been computed using model solid theory. The interband emission energy and the oscillator strength of a strained $GaAs_{1-x}P_x/GaAs_{0.6}P_{0.4}$ quantum dot have been investigated in the presence of a magnetic field, the geometrical confinement and the phosphorous alloy content. We hope that the present investigations would help to guide the future investigations of experimental works on optical switches, efficient diode lasers, modulation doped high mobility field effect transistors, and the phase modulators based on III-V heterostructures.

References

[1] B. R. Bennett, R. A. Soref, and J. A. D. Alamo, IEEE J. Quantum Electron. **26**, 113 (1990).
[2] J. P. Donnelly *et al.*, IEEE J. Quantum Electron. **21**, 1147 (1985).
[3] J. Manning, R. Olshansky, and C. B. Su, J. Quantum Electron. **19**, 1525 (1983). doi: 10.1109/JQE.1983.1071749
[4] G. N. Koskowich and M. Soma, IEEE Electron Device Lert. **9**, 433 (1988). doi: 10.1109/55.6936
[5] C. Mailhiot and D. L. Smith, Phys. Rev. B **35**, 1242 (1987). doi: 10.1103/PhysRevB.35.1242
[6] E. P. O'Reilly, Semicond. Sci. Technol. **4**, 137 (1989). doi: 10.1088/0268-1242/4/3/001
[7] D. L. Smith and C. Mailhiot, Phys. Rev. Lett. **58**, 1264 (1987). doi: 10.1103/PhysRevLett.58.1264
[8] F. Agahi, A. Baliga, K. M. Lau, and N. G. Anderson, Appl. Phys. Lett. **68**, 3778 (1996). doi: 10.1063/1.116614
[9] L. P. Avakyants, P. Yu. Bokov, T. P. Kolmakova, and A. V. Chervyakov, Semiconductors **38**, 1384 (2004). doi: 10.1134/1.1836057
[10] O. S. Gorya *et al.*, Zh. Prikl. Spektrosk. **62**, 160 (1995).
[11] X. Zhang, Y. Shiraki, H. Yaguchi, K. Onabe, and R. Ito, J. Vac. Sci. Technol. B. **12/4**, 2293 (1994). doi: 10.1116/1.579201
[12] X. Zhang *et al.*, Appl. Phys. Lett. **66(2)**, 186 (1995).
[13] Götz Erbert *et al.*, IEEE J. Quantum Electron. **5**, 1077 (1999).
[14] L. Zhong and X. Ma, Jap. J. Appl. Phys. **47**, 7026 (2008). doi: 10.1143/JJAP.47.7026
[15] D. Sun and D. W. Treat, IEEE Photonics Technol. Lett. **8**, 13 (1996). doi: 10.1109/68.475762
[16] C. J. van der Poel *et al.*, Appl. Phys. Lett. **63**, 2312 (1993). doi: 10.1063/1.110510
[17] C. Simserides, J. Phys. Condens. Mat. **11**, 5131 (1999) doi: 10.1088/0953-8984/11/26/314; R. Winkler, D. Culcer, S. J. Papadakis, B. Habib, and M. Shayegan, Semicond. Sci. Technol. **23**, 114017 (2008). doi: 10.1088/0268-1242/23/11/114017
[18] P. Harrison and Q. Wells, *Wires and Dots*, (Wiley, Chichester, 2005). doi: 10.1002/0470010827
[19] O. Voskoboynikov, O. Bauga, O. P. Lee, and O. Tretyak, J. Appl. Phys. **94**, 5891 (2003). doi: 10.1063/1.1614426
[20] G. Martin *et al.*, J. Appl. Phys. Lett. **65**, 610 (1994).
[21] G. E. Pikus and G. L. Bir, *Symmetry and Strain-Induced Effects in Semiconductors*, (Wiley, New York, 1974).
[22] S. L. Chuang, *Physics of optoelectronic devices*, (John Wiley & Sons, New York, 1995).
[23] A. Baliga, D. Trivedi, and N. G. Anderson, Phys. Rev. B **49**, 10402 (1994). doi: 10.1103/PhysRevB.49.10402
[24] J. Simon *et al.*, Phys. Rev. B **68**, 035312 (2003). doi: 10.1103/PhysRevB.68.035312
[25] B. Szafran, B. Stébé, J. Adamowski, and S. Bednarek, Phys. Rev. B **66**, 165331 (2002). doi: 10.1103/PhysRevB.66.165331
[26] C. Xia, Z. Zeng, Z. S. Liu, and S. Y. Wei, Physica B **405**, 2706 (2010). doi: 10.1016/j.physb.2010.03.056
[27] A. D. Yoffe, Adv. Phys. **50**, 1 (2001). doi: 10.1080/00018730010006608
[28] A. Sali, H. Satori, M. Fliyou, and H. Loumrhari, Phys. Stat. Solidi (b) **232**, 209 (2002). doi: 10.1002/1521-3951(200208)232:2<209::AID-PSSB209>3.0.CO;2-O
[29] S. I. Pokutnii, Semiconductors **44**, 488 (2010). doi: 10.1134/S1063782610040147
[30] B. Gil, Nanotechnology **12**, 466 (2001). doi: 10.1088/0957-4484/12/4/317
[31] J. C. Garcia *et al.*, J. Cryst. Growth **175**, 1265 (1997). doi: 10.1016/S0022-0248(96)01017-2